Title

Effect of Molecular-Scale Features on the Polymer Coil Size of Model Viscosity Index Improvers

Journal

Tribology Letters, 62(2)

ISSN

1023-8883

Authors

Ramasamy, Uma Shantini

Lichter, Seth

Martini, Ashlie

Publication Date

2016-05-01

DOI

10.1007/s11249-016-0672-0

Ramasamy US, Lichter S and Martini A (2016) "Effect of Molecular-Scale Features on the Polymer Coil Size of Model Viscosity Index Improvers", Tribology Letters, 62, 23. DOI: 10.1007/s11249-016-0672-0.

Effect of Molecular-Scale Features on the Polymer Coil Size of Model Viscosity Index Improvers

Uma Shantini Ramasamy · Seth Lichter · Ashlie Martini

Received: date / Accepted: date

Abstract Temperature-induced changes in coil size have been proposed as the mechanism underlying the functionality of viscosity index improving polymers. Here, molecular dynamics simulations are used to characterize the effect of temperature on the coil size of model additive polymers. The simulations reproduce experimental observations, where only some polymers increase in size with increasing temperature. The results also reveal that the presence of oxygen atoms in the polymer structure is a key factor in determining whether the polymer expands or contracts. This new simulation approach provides a general methodology for investigating temperature-induced coil size changes in polymeric lubricant additives.

Keywords VI improvers · Polymers · Coil size · Temperature effects

1 Introduction

Viscosity index (VI) improvers are an important class of additives that decrease the change of fluid viscosity with temperature [1,2], enabling optimum lubricant performance over a wider range of operating temperatures. These additives are typically high molecular weight polymers [3–5], such as olefin

Uma Shantini Ramasamy
School of Engineering, University of California Merced, Merced, CA, USA

Seth Lichter
Northwestern University, Department of Mechanical Engineering, Evanston, IL, USA

Ashlie Martini
School of Engineering, University of California Merced, Merced, CA, USA
Tel.: 209-228-2354
E-mail: amartini@ucmerced.edu

copolymer, polyalkylmethacrylates, polyisobutylenes, styrene block copolymer, and ethylene alpha olefin copolymers [1,4,6]. Over the years, advancements in VI technology have been focused on either modifying chemistries [7–9] or manipulating the structure and architecture [10–12] of traditional VI polymers. These variations not only improve viscosity index performance, but in some cases also boost shear, thermal, and oxidative stability of the lubricating oil [7,11–13].

The mechanism behind the functionality of VI additives is still poorly understood. The most commonly accepted theory is the coil expansion mechanism, which was first introduced in 1958 by Selby [14]. Based on this theory, it is proposed that at lower temperatures, the polymer is poorly soluble in the lubricating oil and tends to stay in a coiled conformation. In this state, the polymer does not contribute much to fluid viscosity. At elevated temperatures, the solubility of the polymer in the lubricating oil improves. The polymer expands and induces a thickening effect on the solution, therefore reducing the decline of fluid viscosity with temperature. While this idea is widely accepted in the literature [1,3–5,10,15,16], there is little direct evidence to support it.

Several studies have been performed to evaluate the proposed coil expansion theory [17–20]. In these studies, changes in the size of a polymer coil in solution can be determined using direct or indirect measurement methods. In the direct approach, experimental techniques, such as small angle neutron scattering, static laser light scattering, dynamic laser light scattering, or size exclusion chromatography, are used to measure coil size [17,18]. The indirect methods infer polymer coil size from measured viscosity data, sometimes using empirical correlations, such as Einstein's equation or the Flory-Fox equation [18–21]. These studies have shown that not all VI polymers exhibit coil expansion with increased temperatures [17–20]. In fact, the coil size of some VI polymers, such as olefin copolymers, hydrogenated diene copolymers, and styrene butadiene copolymers, remain constant or decrease with increasing temperature. So far, only VI additives derived from polyalkylmethacrylate chemistry appear to comply with the classical theory, where the coil size of the polymer increases with increasing temperature [17–20]. However, although coil expansion may not be necessary for VI improvement, it has been suggested that polymers that expand are likely to have higher VI contributions than those that do not [17]. Therefore, understanding which polymers expand with temperature and why is important to VI improver technology.

In this work we explore trends in polymer coil size using molecular dynamics (MD) simulation. We use MD simulations to observe and characterize temperature-induced changes in the radius of gyration for several model VI polymers. MD predicted trends are compared to experimental data available in literature to partially validate the proposed method. Additionally, the simulations are also used to explore the effects of polymer chemistry on temperature-induced coil size behaviors. Our findings indicate that polymer size at a given temperature depends on specific atomic-scale features and suggests avenues for further exploration of these dependencies.

2 Methods

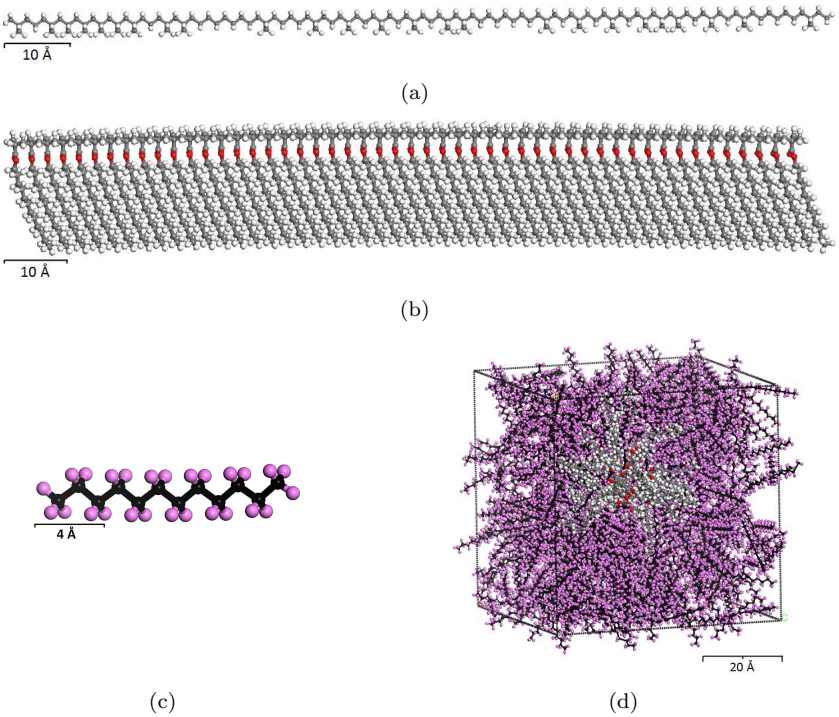

Fig. 1 Atomic structures of the model (a) random ethylene-propylene copolymer, (b) polydodecylmethacrylate polymer, and (c) dodecane. (d) Initial configuration of the polydodecylmethacrylate molecule in dodecane solvent, where the dotted black lines indicate the periodic boundary. For all figures, colored spheres represent individual atoms: grey/black-carbon, white/pink-hydrogen, and red-oxygen

Two model VI additives, random ethylene-propylene copolymer (OCP) and polydodecylmethacrylate (PMA), illustrated in Fig. 1(a) and (b), are used in this work. To compromise between computational efficiency and realism, we chose 50 repeat units as the polymer length. At these lengths, OCP has a molecular mass of 1755.39 g/mol and PMA has a molecular mass of 12722.7 g/mol. The OCP model is constructed with 50/50 mole ratio of ethylene to propylene monomers. Each model VI polymer is placed in a dodecane solvent, as illustrated in Fig. 1(c). The initial configurations of all models are constructed with Accelrys Materials Studio©; a representative image of PMA in dodecane is shown in Fig. 1(d). Subsequent simulations are implemented using Large Atomic/Molecular Massively Parallel Simulation (LAMMPS) software [22]. The simulation systems have periodic boundary conditions with initial dimensions of 6.0 nm × 6.0 nm × 6.0 nm. The All Atom Optimized Potentials

for Liquid Simulations (OPLS-AA) force field [23] with a global cutoff of 1.2 nm is used to describe bond, angle, torsion, and non-bonded interactions (van der Waals and coulombic) between all atoms. A Nośe-Hoover thermostat and barostat are used to control temperature and pressure. All simulations are run with a time step of 1.0 fs and a 1-4 intramolecular (van der Waals and coulombic) scaling factor of 0.0. The scaling factor allows us to modify the pairwise energy contributions between pairs of atoms that are covalently bonded to each other. The van der Waals and coulombic interactions between 1-4 atom pairs, which are those separated by three bonds, are turned off by setting the 1-4 intramolecular scaling factor to zero. Turning off the 1-4 intramolecular interactions increases the prediction accuracy of liquid state properties for molecules with 12 carbons or more [24].

The simulations have three stages, relaxation, equilibration and production, as shown in Table 1. First, the simulation is run under NVT conditions (constant number of atoms, volume, and temperature) at a high temperature to rapidly relax the system. Next the simulations are equilibrated under NPT conditions (constant number of atoms, pressure, and temperature) at 40°C and 100°C, but no data is collected. Lastly, during the production stage, the simulation continues to run under NPT conditions, but data is collected for further analysis.

Table 1 Outline of the various stages of the simulations

Process	Ensemble	Pressure (atm)	Temperature (°C)	Time (ns)
Relaxation	NVT	-	727	0.5
Equilibration	NPT	1.0	40 or 100	3.0
Production	NPT	1.0	40 or 100	100.0

The polymer size, which is calculated throughout the production simulation, is quantified by its radius of gyration, R_g, from the following formula.

$$R_g = \sqrt{\frac{1}{M}\sum_i m_i(r_i - r_{cm})^2}, \tag{1}$$

where M is the total mass of the molecule, m_i is the mass of atom i, r_i is the position of atom i, and r_{cm} is the center of mass of the molecule. The R_g varies over time as the polymer moves and changes its conformation, as presented in Fig. 2(a). Therefore, the raw data is used to plot frequency histograms, Fig. 2(b), that capture the recurrence of specific conformations. A Gaussian function is then fit to the histograms to quantify the mean, μ, and standard deviation of the distributions. While the Gaussian function may not be the best fit for all histograms, it provides a reasonable means to quantitatively compare the differences between different models and temperatures. Lastly, the percent change in the polymer coil size with temperature is estimated from the mean of the distribution using $(\mu_{100^\circ C}\text{-}\mu_{40^\circ C})/\mu_{40^0 C} \times 100$.

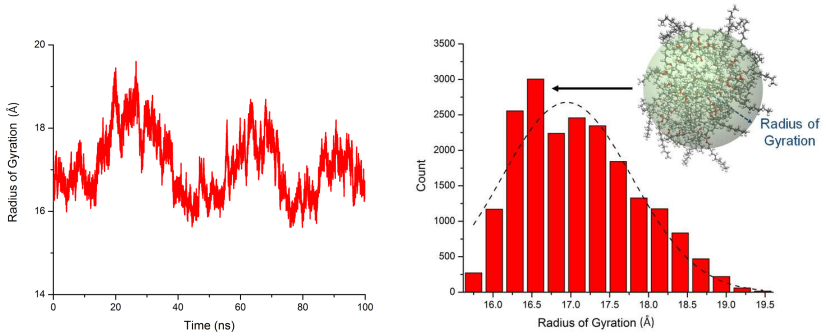

(a) (b)

Fig. 2 (a) Changes in R_g over time as the polymers moves and changes conformations (b) Frequency histogram plotted from raw R_g data. The dotted line represents a Gaussian fit to the histogram data.

3 Results and Discussion

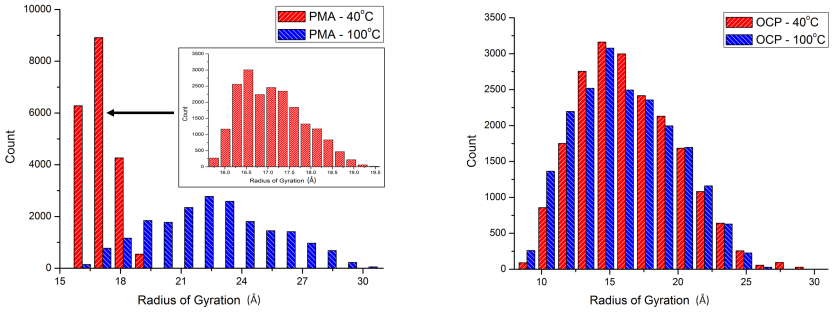

(a) (b)

Fig. 3 Frequency histograms of (a) PMA and (b) OCP at 40°C and 100°C. Gaussian functions are fit to these histograms to obtain information on the mean and standard deviation of the distribution

Fig. 3 shows the frequency histograms for PMA and OCP at 40°C and 100°C. The mean and standard deviation of the Gaussian fit to the distributions are reported in Table 2. The mean R_g of PMA clearly increases when temperature is increased, which means that this polymer is experiencing an increase in coil size with temperature. The standard deviation of PMA is also larger at 100°C compared to 40°C (3.0 vs. 0.7), implying that PMA is able to assume more conformations at the higher temperature. The mean R_g of OCP, on the other hand, has a similar value at both low and high temperatures, indicating that the coil size of OCP does not change significantly with

temperature. The standard deviation of the OCP R_g is also similar at both temperatures (3.6 vs. 3.7), indicating that this polymer has similar number of available conformations at high and low temperatures.

Table 2 Mean and standard deviation of the R_g distribution for PMA and OCP as well as the percent change in the coil size with increased temperature. The figures are representative snapshots of the PMA and OCP simulations at 40°C and 100°C

Temperature (°C)	PMA (Å)	OCP (Å)
40	17.1 ± 0.7	16.5 ± 3.6
	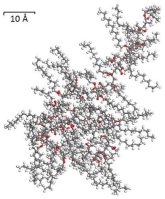	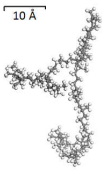
100	22.5 ± 3.0	16.1 ± 3.7
	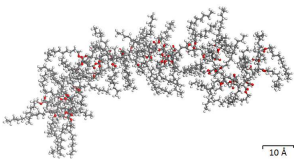	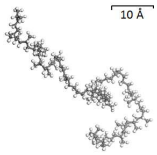
Change (%)	31.5	-2.2

Table 2 also reports the percent change in polymer coil size with temperature. PMA has a positive percent change while OCP has a negative percent change when temperature is increased from 40°C to 100°C. This trend reflects coil size expansion for PMA and slight coil size contraction for OCP. It should be noted that the observed coil size changes for PMA and OCP are specific to the range of temperatures and ambient pressure in our simulations. It is possible that these polymers may exhibit different behaviors under other conditions.

Changes in the coil size of PMA and OCP in a dodecane solvent have been recently studied using small angle neutron scattering [17]. The study reported that the size of PMA increased with temperature (by 6.2 or 11.6%, depending on the type of alkylmethacrylate monomer used), while the size of OCP decreased with temperature (-10.5%). These trends are comparable to our MD predicted results, in which PMA showed a positive percent change and OCP showed a negative percent change. The difference in the magnitude of the change between simulation and experiment may be due to variations in the size and structure of the VI polymers used in our work and in Ref.[17]. Similar trends were also observed in other studies for multiple variations of PMA and OCP chemistries [17–20].

The two most significant differences between PMA and OCP are the presence of long side chains and oxygen atoms on PMA. To study the effects of these structural and chemical properties, several model test polymers were constructed. These models may not represent feasible VI polymers, however they provide insight into the contribution of specific molecular features and chemistries on the functionality of VI polymers. For uniformity, all molecules are 50 repeat units long, placed in a dodecane solvent, and treated according to the process described in the Methods section.

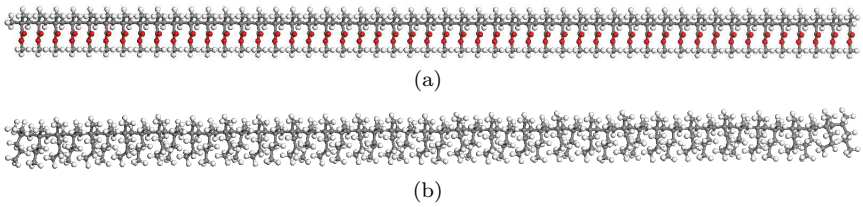

Fig. 4 Molecular structures of (a) polymethylmethacrylate (PMMA) and (b) a test polymer that is structurally similar to PMMA but without oxygen atoms (OFP). For both figures, colored spheres represent individual atoms: grey-carbon, red-oxygen, and white-hydrogen. The scale bar applies to all figures

One of the major differences between PMA and OCP is the presence of long side chains in PMA. For acrylate chemistry, long side chains improve the solubility of the polymer in the lubricating oil [4]. However, there is a possibility that these side chains also influence the overall change in polymer coil size with temperature. To understand the impact of side chain length on polymer coil size, we create a model polymethylmethacrylate (PMMA) which, as shown in Fig. 4(a) (molecular mass 5007.87 g/mol), has much shorter side chains than PMA. The mean and standard deviation of the radius of gyration distribution of PMMA along with the percent change in the polymer coil size are reported in Table 3. We observe that the mean R_g of PMMA is smaller than PMA at both temperatures, but the changes in size with temperature are comparable (31.5% for PMA and 33.4% for PMMA). This suggests that the length of the side chains affects the size, but does not affect the change in size with temperature for acrylate-based VI polymers.

Table 3 Mean and standard deviation of PMMA and OFP at 40°C and 100°C, along with percent change with temperature

Temperature (°C)	PMMA (Å)	OFP (Å)
40	11.2 ± 0.5	18.5 ± 1.9
100	15.0 ± 3.7	16.9 ± 2.6
Change (%)	33.4	-8.7

Another critical difference between PMA and OCP is the presence of oxygen atoms in the chemistry of the molecule, i.e. acrylate-based VI polymers contain oxygen atoms while olefin copolymers do not. We studied the influence of oxygen atoms on polymer coil size by comparing PMMA, a molecule with oxygen atoms, to a model polymer that is structurally similar to PMMA, but without oxygen atoms. The oxygen atoms in the carbonyl and ester groups in PMMA are replaced by $-CH_2-$ groups to create an oxygen free polymer (OFP), Fig. 4(b) (molecular mass 4210.12 g/mol). Again, the mean and standard deviation of the distribution along with the percent change in the polymer coil size are reported in Table 3. The mean R_g of the distribution of OFP is larger than PMMA at both temperatures. However, OFP has a negative percent change in size when temperature is increased, implying that this polymer contracts with temperature, a behavior which was observed for OCP. This suggests that, for linear chains of similar size and structure, the presence of oxygen atoms in the molecule will significantly influence the response of the polymer coil to temperature.

The role of oxygen in altering the conformations of long-chain polymers has been an object of inquiry since at least 1974 [25]. Here, our results point to oxygen as providing a dominant factor in determining whether the polymer expands or contracts on increase in temperature. PMMA is a polymer that contains oxygen. In contrast, in OFP, the oxygens are removed and replaced by carbon atoms. The changes in length of the oxygen-free polymer, OFP, are qualitatively different from those of the oxygen-containing polymers: on heating, OFP decreases in length, while PMMA increases in length. This indicates that, for the polymers studied here, oxygen may affect a polymer's behavior through its influence on the interaction strength, described in the simulations by Lennard-Jones potential parameters (van der Waals and coulombic interactions), and flexibility, described in the simulations by bond angle and torsion potentials, which leads to polymer expansion on heating. Isolating these effects is part of an ongoing work on this topic.

4 Conclusions

This paper presents a method to estimate changes in polymer coil size of VI polymers using MD simulations. The simulations predict that PMA will increase in size with temperature while OCP will not, observations that are consistent with trends reported in the literature, which were obtained using both direct and indirect measurement methods. To understand the difference in coil size trends of PMA and OCP, we analyzed the structural and chemical disparities between these two molecules using simulations of test polymers to isolate the effects of specific differences. These simulations reveal that the presence of oxygen in PMA is critical to the observed temperature-induced increase in coil size. Overall, the molecular dynamics simulation method presented in this study holds significant promise in understanding a polymer's response to temperature change, an area that is particularly relevant for VI

additives. The ability to anticipate the effect of molecular structure and chemistry on coil size may enable molecular-scale design and optimization of novel VI polymers.

Acknowledgements The authors thank Lelia Cosimbescu, Michael Covitch, and Kieran Trickett for helpful discussions. USR and AM were supported by the U.S. Department of Energy's (DOE) Office of Vehicle Technology (under Contract No. 27029) of the PNNL AOP project. PNNL is a multi-program national laboratory operated by Battelle for DOE under Contract DEAC05-76RL01830. USR and AM also acknowledge the American Chemical Society Petroleum Research Fund (# 55026-ND6) for partial support of this research. This work used the Extreme Science and Engineering Discovery Environment (XSEDE), which was supported by National Science Foundation Grant No. ACI-1053575.

References

1. Canter, N.: Viscosity index improvers. Tribol. Lubr. Technol. **67**(9), 10–22 (2011)
2. Cai, G., Zhang, L., Ma, L., Eli, W.: Synthesis and characterization of polybutylacrylate viscosity index improver with anti-wear function. Lubr. Sci. **27**(4), 209–216 (2015)
3. Stachowiak, G.W., Batchelor, A.W.: Engineering Tribology, Second Edition. Butterworth-Heinemann (2001)
4. Rizvi, S.Q.A.: A Comprehensive Review of Lubricant Chemistry, Technology, Selection, and Design. ASTM International, Baltimore (2009)
5. Ahmed, N.S., Nassar, A.M.: Tribology-Lubricants and Lubrication. InTech, Croatia (2011)
6. Bhushan, B. (ed.): Modern Tribology Handbook, Volume One. CRC Press (2001)
7. Jukic, A., Vidovic, E., Janovic, Z.: Alkyl methacrylate and styrene terpolymers as lubricating oil viscosity index improvers. Chem. Tech. Fuels Oils **43**(5), 386–394 (2007)
8. Mohamad, S.A., Ahmed, N.S., Hassanein, S.M., Rashad, A.M.: Investigation of polyacrylates copolymers as lube oil viscosity index improvers. J. Petrol. Sci. Eng. **100**, 173–177 (2012)
9. Jerbić, I.Š., Vuković, J.P., Jukić, A.: Production and application properties of dispersive viscosity index improvers. Ind. Eng. Chem. Res. **51**(37), 11,914–11,923 (2012)
10. Stöhr, T., Eisenberg, B., Müller, M.: A new generation of high performance viscosity modifiers based on comb polymers. SAE Int. J. Fuels Lubr. **1**(2008-01-2462), 1511–1516 (2008)
11. Wang, J., Ye, Z., Zhu, S.: Topology-engineered hyperbranched high-molecular-weight polyethylenes as lubricant viscosity-index improvers of high shear stability. Ind. Eng. Chem. Res. **46**(4), 1174–1178 (2007)
12. Morgan, S., Ye, Z., Subramanian, R., Zhu, S.: Higher-molecular-weight hyperbranched polyethylenescontaining crosslinking structures as lubricantviscosity-index improvers. Polym. Eng. Sci. **50**(5), 911–918 (2010)
13. Ghosh, P., Das, M.: Synthesis, characterization, and performance evaluation of some multifunctional lube oil additives. J. Chem. Eng. Data **58**(3), 510–516 (2013)
14. Selby, T.W.: The non-newtonian characteristics of lubricating oils. ASLE Trans. **1**(1), 68–81 (1958)
15. Nassar, A.M.: Synthesis and evaluation of viscosity index improvers and pour point depressant for lube oil. Pet. Sci. Technol. **26**(5), 523–531 (2008)
16. Ghosh, P., Das, M.: Study of the influence of some polymeric additives as viscosity index improvers and pour point depressants synthesis and characterization. J. Petrol. Sci. Eng. **119**, 79–84 (2014)
17. Covitch, M.J., Trickett, K.J.: How polymers behave as viscosity index improvers in lubricationg oils. Adv. Chem. Engineer. Sci. **5**(02), 134–151 (2015)
18. Mary, C., Phillipon, D., Lafarge, L., Laurent, D., Rondelez, F., Bair, S., Vergne, P.: New insight into the relationship between molecular effects and the rheological behavior of polymer-thickened lubricants under high pressure. Tribol. Lett. **52**(3), 357–369 (2013)

19. Müller, H.G.: Mechanism of action of viscosity index improvers. Tribol. Int. **11**(3), 189–192 (1978)
20. LaRiviere, D., Asfour, A.F.A., Hage, A., Gao, J.Z.: Viscometric properties of viscosity index improvers in lubricant base oil over a wide temperature range. Part I: Group II base oil. Lubr. Sci. **12**(2), 133–143 (2000)
21. Münstedt, H., Schwarzl, F.R.: Experimental methods to determine molecular quantities. In: Deformation and Flow of Polymeric Materials, pp 43–76. Springer, Heidelberg (2014)
22. Plimpton, S.: Fast parallel algorithms for short-range molecular dynamics. J. Comp. Phys. **117**(1), 1–19 (1995)
23. Jorgensen, W., Maxwell, D., Tirado-Rives, J.: Development and testing of the opls all-atom force field on conformational energetics and properties of organic liquids. J. Am. Chem. Soc. **118**(45), 11,225–11,236 (1996)
24. Ye, X., Cui, S., de Almeida, V.F., Khomami, B.: Effect of varying the 1-4 intramolecular scaling factor in atomistic simulations of long-chain n-alkanes with the opls-aa model. J. Mol. Model **19**(3), 1251–1258 (2013)
25. Dale, J.: The conformational consequences of replacing methylene groups by ether oxygen. Tetrhedron **30**(12), 1683–1694 (1974)